A 500MHz Low Phase-Noise AlN-on-Silicon Reference Oscillator

Hossein Miri Lavasani, Reza Abdolvand, and Farrokh Ayazi

School of Electrical and Computer Engineering, Georgia Institute of Technology, Atlanta, GA 30332

***Abstract*-This paper presents a 496MHz low phase-noise reference oscillator using a high-Q lateral-mode AlN-on-Si micromechanical resonator that does not require DC voltage for operation. The sustaining amplifier consists of an inductorless high-gain CMOS transimpedance amplifier (TIA) that is optimized for low phase-noise. The resonator is designed to have a high quality factor in air (Q~3800) with low motional impedance. The measured phase-noise at 1kHz offset is –92dBc/Hz with phase-noise floor below –147dBc/Hz (exceeding GSM phase-noise requirement by 2dB and 28dB, respectively).**

I. INTRODUCTION

Frequency reference oscillator is a critical component of any radio transceiver. Currently, most reference oscillators are based on quartz crystals. Although quartz oscillators exhibit superior stability and phase-noise performance, their frequency limitation (<200MHz) reduces the performance of multi-mode RF transceivers because of the increase in the up-conversion ratio for the synthesizers. Moreover, the inherent incompatibility of quartz with IC fabrication prevents size reduction in transceivers. On the other hand, Silicon-integrated micromechanical oscillators offer small form factor, higher frequency operation, and integration with electronics [1]-[3].

Prior work on low phase-noise silicon micromechanical reference oscillators are based on capacitive MEMS resonators with native frequencies in the VHF range [3], [4]. The motional impedance associated with high-frequency (>100MHz) capacitive resonators is usually large (>10kΩ). In addition, capacitive resonator need to be operated in vacuum and require a DC polarization voltage that is typically beyond what is available in standard IC processes (>5V). This complicates the realization of low-power low-phase-noise UHF oscillators. Laterally-excited thin-film piezoelectric-on-substrate (TPoS) micromechanical resonators, on the other hand, offer an alternative solution as they exhibit significantly lower motional impedances (<1kΩ) at UHF range [5]. In addition, unlike thickness-mode piezoelectric technology (i.e., FBAR), multiple frequency resonators can be integrated on the same substrate.

In this work, we demonstrate a 496MHz reference oscillator based on an AlN-on-Si TPoS resonator. By including silicon in the resonant structure, most of the acoustic energy is stored in a low-acoustic-loss material (single crystal silicon). This boosts the quality factor of the resonator, a key performance parameter for oscillator application, when compared to a fully piezoelectric resonator (e.g., FBAR). The frequency of the resonator, fabricated on an SOI wafer, is defined by its lateral dimensions through photolithography. The buried oxide layer of the SOI wafer has a large positive temperature coefficient of frequency (TCF) and can be optionally preserved at the bottom of the resonant structure to compensate for the negative TCF of the other material in the stack, resulting in a temperature stable oscillator [6]. As shown in Fig. 1, the resonator structure resembles a block designed to operate in high order width-extensional resonance mode. The measured motional impedance of the device is ~600Ω and the unloaded Q is ~3800 measured in air. The fabrication process flow of this type of TPoS resonators is low-temperature and post-CMOS-compatible, adding more value to this approach. The piezoelectric resonator is fabricated in Georgia Tech's Microelectronics Research Center using AlN films deposited by Advanced Modular Sputtering Inc.

The measured phase-noise of the oscillator is –92dBc/Hz at 1kHz offset and –147dBc/Hz far-from-carrier. The TIA was fabricated in a 1P6M 0.18um CMOS process. To the authors' knowledge, this is the highest frequency reference oscillator based on laterally-excited MEMS piezoelectric resonators.

II. OSCILLATOR BLOCK DIAGRAM

The block diagram of the reference oscillator is shown in Fig. 1. The frequency of oscillation is determined by a 496MHz high-Q piezoelectric resonator.

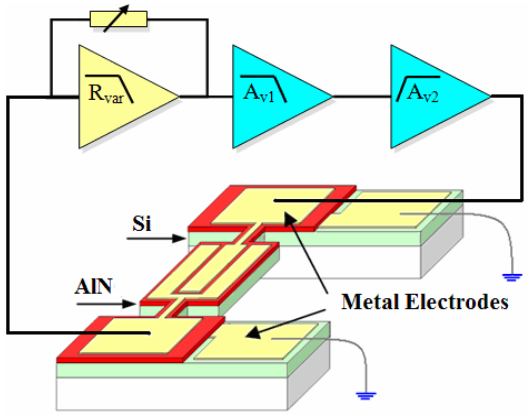

Fig. 1. Block diagram of the piezoelectric oscillator.

The sustaining amplifier consists of two parts: TIA with tunable gain and two subsequent voltage amplifiers. The gain tuning is achieved by an NMOS resistor. The third stage helps relax gain constrains on the previous gain stage; thereby, reducing the power consumption and improving linearity. Due to large power-handling of these resonators (>10dBm), automatic level control (ALC) is not necessary.

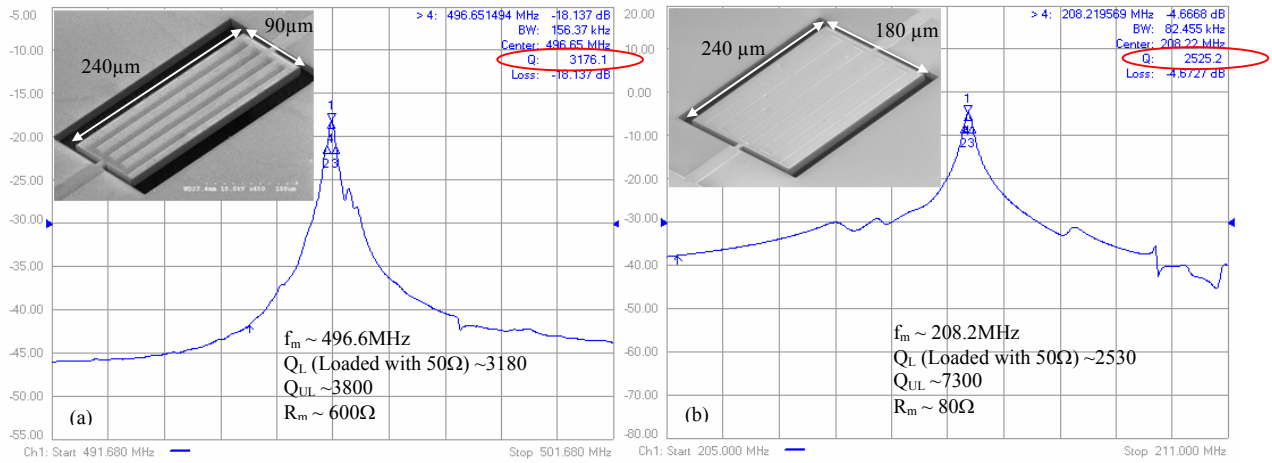

Fig. 2. SEM view and frequency response of (a) 496MHz, (b) 208MHz AlN-on-Si resonators

III. RESONATOR DESIGN AND FABRICATION

The resonator used in the oscillator is a 9th-order TPoS lateral bulk acoustic resonator. A thin layer of sputtered AlN sandwiched between two metal electrodes is used as the transduction mechanism on top of the silicon device layer on an SOI substrate (Fig. 1). The high electromechanical coupling of the piezoelectric transduction combined with the low acoustic loss of the single crystal silicon substrate provides high Q resonators with low motional impedance. The linearity of the resonator is also improved due to the high energy density of the silicon layer. This combination makes TPoS resonators an excellent candidate for high frequency oscillator applications. The detailed explanation of the fabrication process can be found in [7].

The finger pitch size is 10µm for 496MHz device and 20 µm for 208MHz device. Out-of-phase strain field induced in the two electrodes at resonance causes a 180º phase shift in the signal. The frequency is reduced more than 20/10 ratio due to the increase in finger width.

The frequency response of the device is measured in air using an Agilent E8364B VNA with GSG probes (Fig. 2). Since the termination load of the network analyzer (50Ω) is comparable with the motional impedance of both device (~80 Ω and 600Ω) the Q values measured (~2520 and ~3180) are evidently lower than the unloaded Q of the resonator (~7400 and ~3800).

IV. SUSTAINING AMPLIFIER DESIGN AND OPTIMIZATION

A. Transimpedance Amplifier Design

To realize an oscillator in the UHF range using a lossy micromechanical resonator with large input/output parasitic capacitance (~2pF), it is crucial to use high-gain broadband TIA. To this end, a three-stage TIA with variable gain at the first stage is designed (Fig. 3). The TIA was intended to be a universal design, capable of sustaining oscillation with a broad range of resonators having characteristics of: 100MHz < f < 1GHz and 50Ω < R_m < 1kΩ.

To achieve high gain while maintaining the wideband characteristic of the TIA, a low-gain transimpedance stage is followed by two wideband voltage gain stages. Shunt-shunt feedback is introduced in each voltage gain stage to reduce the impedance at the inter-stage nodes. This technique increases the frequencies of the poles resulting from the inter-stage nodes to much higher than those of the input/output; thus providing wideband characteristic without increasing the power consumption. Another advantage of this technique is to eliminate on-chip inductors typically used in high-gain gigabit CMOS TIA circuits to enhance the bandwidth. The result is significant reduction in area.

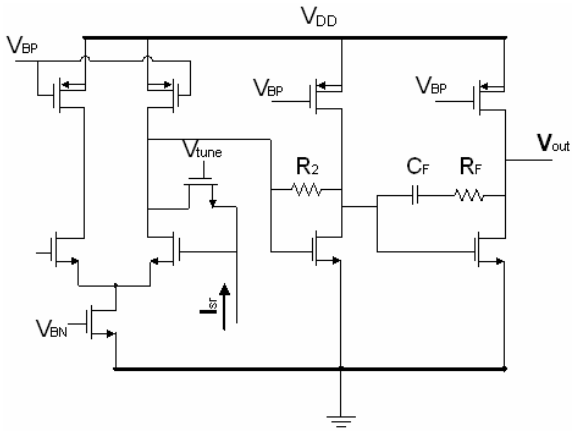

Fig. 3. Schematic diagram of the TIA (biasing not shown)

The designed TIA achieves the -3dB bandwidth of more than 880MHz at maximum gain (72dBΩ) when loaded with 2pF capacitance load at the input and output node.

The main reason to choose common source over higher gain topologies such as cascode is to increase the voltage swing and enable the circuit to operate from lower supply (in this case 1.5V) that further reduces the power consumption. The higher output swing results in lower phase-noise floor as the dynamic range of the TIA will be improved.

To boost the gain at higher frequencies, capacitive coupling is used in the third stage. The high pass response of the third stage significantly attenuates the low frequency noise of the amplifier, which is higher in CMOS circuits due to large flicker noise. Therefore, the contribution of TIA noise to the

overall close-to-carrier phase-noise is reduced. The choice of capacitor C_F determines the attenuation. For the case of 2pF, the phase-noise at 1kHz offset is 2dB lower than the oscillator constructed with the same resonator but using the TIA without capacitive coupling.

B. Phase-noise Optimization

The phase-noise of the oscillator can be categorized into three regions: close-to-carrier (f_{off} < 10kHz), intermediate (10kHz< f_{off} < 600kHz), and far-from-carrier (f_{off} > 600kHz).

In the close-to-carrier region, the dominant factor in determining the phase-noise of the oscillator is Q of the resonator [3]. The phase-noise in this region is mainly due to the up-conversion of 1/f noise of the TIA.

The phase-noise in the lower end of the intermediate region (10kHz < f_{off} <100 kHz) is dominated by the up-conversion of thermal noise. The noise in this region and close-to-carrier region can be modeled by (1).

Assuming a simple lumped series RLC electrical model for the resonator, close-to-carrier phase-noise of the oscillator can be approximated [5] as

$$L(f_m) = \frac{FkT_0}{2P_o}\left[1+\frac{1}{f_m^2}\left(\frac{f_{off}}{2Q_L}\right)^2\right]\left(1+\frac{f_\alpha}{f_m}\right) \qquad (1)$$

Where f_m, f_{off}, f_α, F, P_o are the oscillation frequency, offset frequency, a constant related to 1/f noise corner, noise figure of the TIA, and oscillation power, respectively. Q_L, called loaded Q, is defined as

$$Q_L = Q_{UL}\frac{R_m}{R_m + R_{in} + R_{out}} \qquad (2)$$

Where Q_{UL}, R_m, R_{in}, R_{out} are unloaded Q of the resonator, motional impedance of the resonator, input, and output resistance of the TIA, respectively.

It can be seen that the phase-noise is inversely proportional to Q_L. To optimize the phase-noise, input/output impedances of the TIA have to be minimized.

The upper end of the intermediate region (100kHz < f_{off} < 600kHz) is where transition between close-to-carrier and far-from-carrier region takes place. The Leeson frequency, f_L, can be approximated by (3). In this case, f_L will be around 600kHz, consistent with the extracted value from the phase-noise plot (~600kHz).

$$f_L \sim \frac{f_m}{2Q_{UL}} \qquad (3)$$

Far-from-carrier region (f_{off} > 600 kHz) is the phase-noise floor of the oscillator that is limited by the TIA and off-chip 50Ω buffer noise.

In addition to the noise from the electronics, mechanical phenomena such as particle absorption and thermal gradient contribute to the phase-noise at very low offset frequencies (f_{off} < 10Hz). Moreover, the frequency shift caused by parasitic capacitance at input and output node has negative effect on the phase-noise.

V. MEASUREMENT RESULTS

The TIA and biasing circuitry is fabricated in a 0.18um 1P6M CMOS process. Another TIA that does not incorporate capacitive coupling was also fabricated on the same die for the purpose of performance comparison. An off-chip 50Ω buffer is used to interface with the measurement equipments. The TIA was measured to have maximum transimpedance gain of more than 71.8dBΩ and maximum -3dB bandwidth in excess of 960MHz when loaded with 2pF at both input and output nodes. The TIA -3dB bandwidth when interfaced with standard photodiodes with equivalent capacitance ~500fF will be enhanced to 1.5GHz. The TIA gain could be varied by 8dB (Fig. 4). The amplifier and biasing circuitry consumed 6.2mA from 1.5V supply. The die size is 1mm^2 of which 450µm × 330µm is occupied by the sustaining amplifier (Fig. 5).

The measured phase-noise of the oscillator in air is –92dBc/Hz at 1kHz offset and below –147dBc/Hz at far-from-carrier (Fig. 6). The measurement was carried out by an Agilent EE5500 phase-noise analyzer. The oscillation power was 1.9dBm, well within the resonator linear range. The slight degradation in phase-noise performance around 100kHz offset is due to the internal phase-noise limit (~–136dBc/Hz) of the Agilent E8257C Analog Signal Generator that is used in the phase-noise measurement setup. The spurs below 1kHz are caused by 60Hz signal and its harmonics.

To demonstrate the effect of Q loading on the phase-noise of the oscillator, a 208MHz AlN-on-Si resonator that exhibits Q_{UL} ~ 7400 and R_m ~80 Ω was interfaced with the same TIA. The oscillation power was 5dBm. The measured phase-noise at 1kHz offset was –95dBc/Hz and phase-noise floor –152dBc/Hz. While more than 5dB improvement to the phase-noise floor can be explained by the lower motional impedance of the resonator, the less than expected improvement in close-to-carrier phase-noise can be explained by the fact that in both cases, Q_L is roughly the same. Considering R_{in} ~ 100Ω and R_{out} ~ 120Ω, Q_L is 2300 for this device whereas for the case of 496MHz resonator, Q_L is more than 2500. The 3dB difference in phase-noise is due to the fact that the oscillation power for 208MHz is ~3dB higher.

As described in section IV, the phase-noise of the oscillator (especially close-to-carrier) is a strong function of the Q of the resonator. Although piezoelectric resonators exhibits lower Q than capacitive resonators, the availability of low-impedance piezoelectric resonators at much higher frequencies [5] make it possible to realize oscillators that operate at frequencies 5 to 10 times than those based on capacitive resonators. The reduction in up-conversion ratio compensates for close-to-carrier phase-noise of the oscillator. Another advantage is the elimination of costly and complex vacuum packaging due to the fact that unlike lower frequency capacitive resonators, Q of high frequency piezoelectric resonators will not be limited by air damping.

To better understand this issue, the phase-noise of the oscillator in this work has been scaled to the appropriate frequency and compared with the state-of-the-art oscillators based on capacitive resonators [3], [4] (Table I). While the

close-to-carrier phase-noise is comparable with those of capacitive-based oscillators, far-from-carrier floor is much lower thanks to the down-conversion ratio of 5-8. A summary of the oscillator specification can be found in Table II.

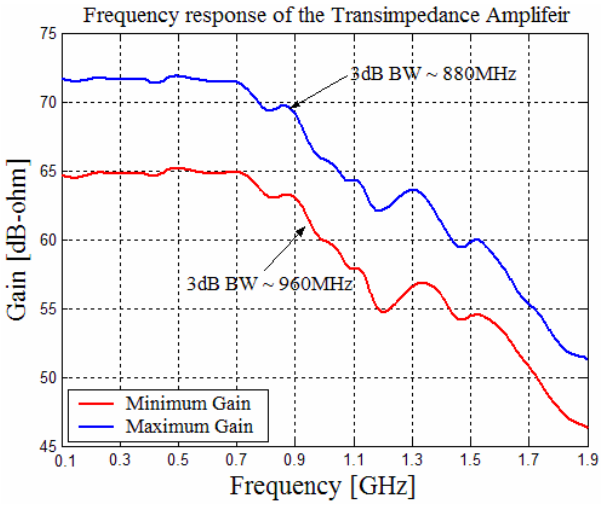

Fig. 4. Frequency response of the tunable TIA

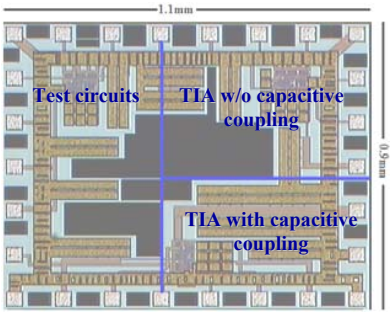

Fig. 5. Micrograph of the fabricated die

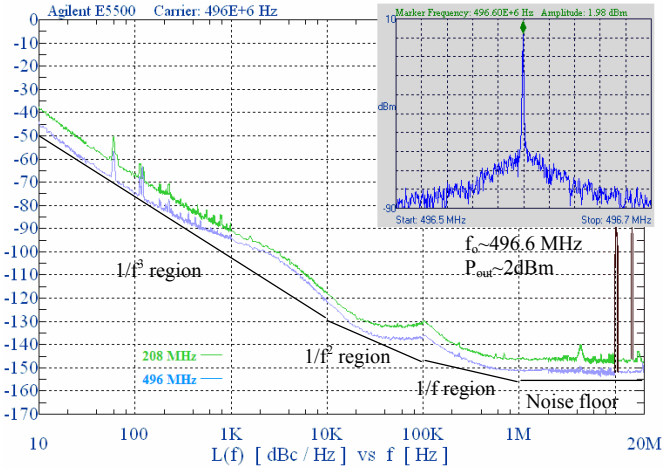

Fig. 6. Measured phase-noise of 496MHz and 208MHz oscillators. The spectrum of output waveform for 496MHz is also shown.

VI. CONCLUSION

A 496MHz oscillator based on an AlN-on-Si TPoS resonator has been presented, which to the authors' knowledge is the highest frequency MEMS oscillator reported that uses a *lateral-mode* micromechanical resonator. Unlike capacitive MEMS resonators, the AlN-on-Si resonator does not require a DC voltage for operation. An inductorless high-gain broadband CMOS TIA has been designed to interface with the resonator. The effect of Q loading on the phase-noise performance is studied and the approach to minimize its effect on phase-noise is explained.

ACKNOWLEDGMENTS

The authors wish to thank Dr. Krishnakumar Sundaresan for his invaluable help in phase-noise measurement and MOSIS for IC fabrication support through MOSIS Educational Program (MEP).

TABLE I. COMPARISON OF MEMS OSCILLATORS

Oscillator	Disk [4]	SiBAR [3]	This Work		
			61MHz	103MHz	496MHz
PN @ 1kHz (dBc/Hz)	-110	-108	-110	-106	-92
PN @ 10kHz (dBc/Hz)	-128	-120	-136	-132	-118
PN floor (dBc/Hz)	-132	-136	-165	-161	-147
f_m (MHz)	61	103	496		
Resonator Q	48,000	80,000	3,800		
Vacuum	Yes	Yes	No		
DC Voltage	Yes	Yes	No		
IC Process	0.35um	0.18um	0.18um		

TABLE II. OSCILLATOR PERFORMANCE SUMMARY

Sustaining Amplifier	
Maximum Gain (dBΩ)	71.8
Maximum -3dB Bandwidth (MHz)	960
Power (mW)	9.4
Process	0.18um 1P6M CMOS
Resonator	
Technology	Piezoelectric
Q	3800
Motional Impedance (Ω)	600
Oscillator	
Phase-noise @ 1kHz (dBc/Hz)	-92
Phase-noise @ 10kHz (dBc/Hz)	-118
Phase-noise floor (dBc/Hz)	-147
RMS Jitter [100-10MHz] (ps)	0.56

REFERENCES

[1] G. K. Ho, K. Sundaresan, S. Pourkamali, and F. Ayazi, "Temperature-compensated IBAR reference oscillators", Proc. IEEE-ASME MEMS, pp. 910-913, Jan 2006.

[2] S. Lee, M.U. Demirci, and C.T.-C. Nquyen, "A 10-MHz micromechanical resonator Pierce reference oscillator for communications", Proc. Int. Conf. Solid-State Sensors and Actuators, pp. 1094-1097, 2001.

[3] K. Sundaresan, G. K. Ho, S. Pourkamali, and F. Ayazi, "A Low Phase Noise 100MHz Silicon BAW Reference Oscillator", Proc. IEEE CICC, pp. 841-844, Sept 2006.

[4] Y. Lin, S. Lee, S. Li, Y. Xie, Z. Ren, C.T.-C. Nquyen, "Series-Resonant VHF Michromechanical Resonator Reference Oscillators", IEEE J. Solid-State Circuits, vol. 39, no. 12, pp. 2477-2491, Dec 2004.

[5] G. K. Ho, K. Sundaresan, S. Pourkamali, and F. Ayazi, "Low-motional-impedance highly-tunable I2 resonators for temperature-compensated oscillators", Proc. IEEE-ASME MEMS, pp. 116-120, Jan 2005.

[6] R. Abdolvand, H. Mirilavasani, and F. Ayazi, "Low-Voltage Temperature-Stable Micromechanical Piezoelectric Oscillator," To be presented in International conference on Solid-State Sensors, Actuators and Microsystems, June 2007.

[7] R. Abdolvand, G. K. Ho, J. Butler, and F. Ayazi, "ZnO-on-nanocrystalline-diamond lateral bulk acoustic resonators", Proc. IEEE-ASME MEMS, pp. 795-798, Jan 2007.